Optimized Error Diffusion for Image Display [†‡]

B.W. Kolpatzik, C.A. Bouman
School of Electrical Engineering
Purdue University
West Lafayette, IN 47907-0501
phone: 317-494-0340, email: bouman@ecn.purdue.edu

Abstract

Displaying natural images on an 8 bit computer monitor requires a substantial reduction of physically distinct colors. Simple minimum mean squared error (MMSE) quantization with 8 levels of red and green and 4 levels of blue yields poor image quality.

A powerful means to improve the subjective quality of a quantized image is error diffusion. Error diffusion works by shaping the spectrum of the display error. Considering an image in raster ordering, this is done by adding a weighted sum of previous quantization errors to the current pixel before quantization. These weights form an error diffusion filter.

We propose a method to find visually optimized error diffusion filters for monochrome and color image display applications. The design is based on the lowpass characteristic of the contrast sensitivity of the human visual system. The filter is chosen so that a cascade of the quantization system and the observer's visual modulation transfer function yields a whitened error spectrum. The resulting images contain mostly high frequency components of the display error, which are less noticeable to the viewer. This corresponds well with previously

[†]This work was supported by an NEC Faculty Fellowship.
[‡]*Journal of Electronic Imaging*, vol. 1, no. 3, pp. 277-292, July 1992.

published results about the visibility of halftoning patterns. An informal comparison with other error diffusion algorithms shows less artificial contouring and increased image quality.

1 Introduction

High quality color images can be displayed on monitors with 24 bits per pixel by assigning 256 different shades (8 bits) of red, green and blue to each input pixel. Hence, each pixel color is selected out of $2^{24} \approx 16$ million different colors, and the resulting quantization steps are practically invisible to a human observer.

However, many low cost computer and display devices can display only 256 different colors (8 bits) at a time, due to hardware constraints. This requires a substantial reduction of physically distinct colors. Simple minimum mean squared error (MMSE) quantization with 8 levels of red and green and 4 levels of blue yields poor image quality.

A powerful means to improve the subjective quality of a quantized image is error diffusion. The basic algorithm was first introduced by Floyd and Steinberg [1] for halftoning in the printing process of gray scale images. It is based on the observation, that the human visual sensitivity to display errors is dependent on spatial frequency.

Floyd and Steinberg proposed an algorithm that calculates the quantization error for each pixel and feeds it forward to four unquantized pixels of the input image. As shown in [2, 3, 4], this algorithm is equivalent to a feedback system that adds a weighted sum of four previous quantization errors to the current pixel before it is quantized. Since the weighting factors sum to one, it can be shown that the average value of the quantized image is locally equal to the true gray scale value.

Billotet-Hoffmann and Bryngdahl [5] compared the performance of ordered dithering with error diffusion. They concluded that error diffusion, as proposed by Floyd and Steinberg,

yields quantized images that are comparable or superior to most ordered dithering techniques, when nonlinear effects such as dot overlap are not significant. However, the image quality still suffers from visible, correlated artifacts.

Ulichney [6] examined the spectral characteristics of the display error for the error diffusion algorithm using a variety of feedback filters. He proposed an error diffusion filter with randomized weighting coefficients to shape the display error spectrum to have mostly high frequency content ("Blue Noise"). He stated that Blue Noise is less noticeable to a human observer than errors with a white power spectrum. Goertzel [7, 8] applied error diffusion with a randomized error diffusion filter to monochrome and color images. It was found that randomized coefficients remove deterministic (iterative) patterns in the displayed image. Although in comparison to the approach with a deterministic filter, the image quality is improved, false contouring artifacts remain.

The objective of this paper is to develop an optimized algorithm for a specific human visual model. Most previous methods use information about the human visual system only indirectly or qualitatively [2, 10, 11, 12, 13]. To achieve this, a modulation transfer function (MTF) for an overall system in a luminance-chrominance space is defined. This system model includes the effects of spatial sampling due to the monitor and a model for the human modulation transfer function. We assume that each part of this model can be described by three decoupled system functions for luminance and both chrominance components. The error diffusion algorithm is then independently matched to the three components of the resulting system MTF. This is done by choosing an optimized error diffusion filter for each component. It is shown that designing the optimal error diffusion filter corresponds to an optimum 2D linear prediction problem.

One important underlying assumption of our error diffusion filter design method is that the quantization error has a white power spectrum. However, this assumption is not valid

in general. It is important to notice that the quantization error is defined as the difference between the input and output of the quantizer, while the display error is the difference between the input and output of the entire quantizing system. For error diffusion applied to gray scale images, it was found that the whiteness assumption about the quantization error is violated whenever the input gray scale value is close to a quantization level. This often leads to false contouring.

Whiteness of the quantization error spectrum can be assured by combining standard error diffusion with dithered quantization (Dithered Error Diffusion, DED). The method is based on the fact that the quantization error spectrum can be whitened by adding a fixed amount of white noise to the signal before it is quantized. However, this also increases the display error variance. A further refinement of this algorithm is examined, that adds dithering noise locally, based on a nearest neighbors criterion (Locally Dithered Error Diffusion, LDED). With this approach, it is possible to remove false contouring, without adding excessive noise to the image.

Simulations were carried out using visual models from Sullivan [14, 15], Näsänen [16] and Mullen [17], describing the human modulation transfer function and reflecting the lowpass characteristic of the human visual system to changes in luminance and chrominance. The models differ in their cutoff frequencies and their spatial symmetry properties.

Considering a modulation transfer function for the overall system and then designing the error diffusion filter accordingly yields an improvement over the conventional methods of error diffusion. The algorithms were applied to gray scale images as well as to color images and their performance was compared. The best results were achieved using the LDED algorithm. False contours are broken up, without distorting the image through excessive amounts of dithering noise.

Section 2 describes the error diffusion algorithm for monochrome images and the opti-

mization for a given human MTF. Then we extend our analysis to color images. Section 3 discusses the whitening assumption of the quantization error. Some models of the human MTF are described in Section 4 and Section 5 contains experimental results.

2 Optimized Error Diffusion

Section 2.1 briefly describes the basic error diffusion algorithm. Section 2.2 develops our approach for designing an optimized error diffusion filter for the luminance component and Section 2.3 extends the algorithm to color images.

2.1 Basic Error Diffusion

The basic error diffusion algorithm for monochrome images, as it was introduced by Floyd and Steinberg [1] is illustrated in Fig. 1. We will use the analysis given in [3, 4] as the basis for our approach. In our simulations, we process the input image in raster order, starting with the pixel in the upper left corner and proceeding line for line to the lower right corner. Let $n = (n_1, n_2)$ denote the pixel location in the image. Referring to Fig. 1 we write $s(n)$ for pixels of the unquantized input image. In general, $s(n)$ will be linearly proportional to image luminance. Since most image data formats incorporate some nonlinear predistortion (e.g. gamma correction), this requires that the data be transformed back to a linear format before processing. This transformation is important since our models for the human visual system and the display assume that the data is proportional to light intensity.

The input to the quantizer, $\tilde{s}(n)$, is computed by adding a sum of weighted, previous quantization errors, $q(n)$, to the current pixel, $s(n)$. This set of weights forms the error diffusion filter, G, with impulse response, $g(n)$. The output image of our quantizing system

is $y(n)$. We obtain the display error,$e(n)$, as

$$e(n) = s(n) - y(n).$$

The quantization error, $q(n)$, is given by

$$\begin{aligned} q(n) &= \tilde{s}(n) - y(n) \\ &= \sum_{k<n} g(n-k)q(k) + e(n), \end{aligned} \tag{1}$$

where $n - k = (n_1 - k_1, n_2 - k_2)$ and $k < n$ denotes pixels with ($k_1 = n_1$ and $k_2 < n_2$) or $k_1 < n_1$. We define the two dimensional Discrete Time Fourier Transform (DTFT) [18] of $e(n)$ to be

$$E(\omega) = \sum_{n \in \mathbb{Z}^2} e(n) \exp[-jn\omega^T],$$

where $\omega = (\omega_1, \omega_2)$ and $\mathbb{Z}$ is the set of all integers. Then we obtain from (1) a relationship between the spectrum of the display error, $E(\omega)$, and the spectrum of the quantization error, $Q(\omega)$,

$$E(\omega) = Q(\omega)[1 - G(\omega)], \tag{2}$$

where $G(\omega)$ is the frequency response of the error diffusion filter. If we assume that $q(n)$ is spatially uncorrelated, then $Q(\omega)$ is white, and the display error spectrum can be shaped by designing the filter $H(\omega) = 1 - G(\omega)$. In Section 3 we will develop methods to assure that this whiteness assumption holds.

Based on this analysis, the error diffusion filter, $G(\omega)$, is critical in determining the spectrum of the display error. Tab. 1 lists some common examples of error diffusion filters and Fig. 2 shows the location of the filter coefficients. Floyd and Steinberg proposed a filter, $g(n)$, with four positive, deterministic coefficients. Stucki [6] defined a filter that operates on 12 previous quantization errors. Due to space limitations, it is not listed in the table. The coefficients of most error diffusion filters, including the filters from Floyd, Steinberg and Stucki, sum to one. Therefore, $G(\omega = 0) = 1$. It follows from (2) that the DC component of

	$g_{0,1}$	$g_{1,-1}$	$g_{1,0}$	$g_{1,1}$
Floyd-Steinberg	0.4375	0.1875	0.3125	0.0625
Goertzel	z	0	0	1.0-z
1st order LP (non-separable) (luminance)	0.7770	-0.009	0.7861	-0.6098
1st order LP (non-separable) (chrominance)	0.8767	0.0359	0.8205	-0.7376

Table 1: Coefficients of error diffusion filters. For the filter used by Goertzel,z is a random number, uniformly distributed between 0.25 and 0.75.

the display error, $E(\omega = 0) = 0$. This implies that the average gray value of the quantized image, $y(n)$, is locally adjusted to the true gray scale value of the input image. Ulichney [6] and Goertzel [8] examined error diffusion filters with randomized coefficients. In these cases $g(n)$ changes randomly with the location in the image. Tab. 1 lists the coefficients of a filter, used by Goertzel. The parameter z denotes a random number, uniformly distributed between 0.25 and 0.75 and chosen independently for each pixel. As with the deterministic filters, the sum of the coefficients at any location is also equal to one.

The error diffusion filter should be designed so that the display error, $e(n)$, is the least noticeable to a human observer. Since the human visual system is more sensitive to low frequency changes in luminance then to high frequency components, most of the energy of the display error should be shifted to high frequencies. However, forcing the DC component of the display error to zero by setting the sum of the filter coefficients to one is an artificial constraint. Our simulations show that better results can be obtained, by tolerating some display error at zero frequency and distributing the error energy over the entire spectral range according to a human visual model. The next section formulates such a minimization criterion.

2.2 Optimization and Design of the Error Diffusion Filter in Luminance

To design an optimized error diffusion filter, $G(\omega)$, for the luminance component, we consider a model for the overall system, as illustrated in Fig.3. After the error diffusion algorithm and quantization is applied to the input image, the quantized image is converted by a monitor to a spatially continuous signal. It is filtered with the monitor MTF, $P(\Omega)$, where $\Omega = (\Omega_1, \Omega_2)$ and $\Omega_1, \Omega_2 \in (-\infty, \infty)$. This gives rise to aliasing terms in the spectrum. The resulting image is seen by a human observer. It passes through the human visual system with MTF, $W(\Omega)$, and becomes the perceived image. Linearity is assumed for each component of our system.

We would like to minimize $E[\varepsilon^2(x)]$, the energy of the perceived error, by choosing an optimal error diffusion filter. As illustrated in Fig.3a, $\varepsilon(x)$ is the perceived difference between the quantized image, $y(n)$, and the original image, $s(n)$. Since linearity of the monitor and the human MTF is assumed, it is sufficient to consider the difference signal $s(n) - y(n)$ as the input to our system, as shown in Fig.3b. This is the display error, $e(n)$, as it was defined in the previous section.

Assuming that the input image can be viewed as a stationary random process, the perceived error $\varepsilon(x)$ is also a stationary random process and the energy of $\varepsilon(x)$ is given by

$$E[\varepsilon^2(x)] = \frac{1}{4\pi^2} \int_{\Omega \in I\!R^2} \Phi_\varepsilon(\Omega) d\Omega,$$

where $\Phi_\varepsilon(\Omega)$ is the power spectral density of $\varepsilon(x)$.

In Appendix A, we show that the energy of the perceived error can be expressed in terms of the power spectrum of the display error, $\Phi_e(\omega)$ and an equivalent overall system function $\tilde{W}(\omega)$, such that

$$E[\varepsilon^2(x)] = \frac{1}{4\pi^2} \int_{\omega \in I\!P^2} \Phi_e(\omega) \mid \tilde{W}(\omega) \mid^2 d\omega, \tag{3}$$

where $\mathbb{P} = [-\pi, \pi]$, and the overall system function $\tilde{W}(\omega)$ is given by

$$| \tilde{W}(\omega) |^2 = f_s^2 \sum_{l \in \mathbb{Z}^2} | P(\omega f_s + 2\pi l f_s) W(\omega f_s + 2\pi l f_s) |^2,$$

where $l = (l_1, l_2)$ and f_s is the sampling rate of the monitor in cycles/degree. The sampling rate is obtained by taking the reciprocal of the angle of perception of a single displayed pixel, for a fixed viewing distance.

Fig.3c illustrates the resulting simplified system model, where $\tilde{\varepsilon}(n)$ is the output of an equivalent discrete system $\tilde{W}(\omega)$. This simplification results from (3) and the fact that

$$E[\varepsilon^2(x)] = E[\tilde{\varepsilon}^2(n)].$$

Therefore, we can minimize the energy of the perceived error by minimizing the energy of $\tilde{\varepsilon}(n)$. Furthermore, from (2) it follows that

$$\Phi_e(\omega) = \Phi_q(\omega) \mid 1 - G(\omega) \mid^2 .$$

Replacing $\Phi_e(\omega)$ in (3), we want to minimize

$$E[\tilde{\varepsilon}^2(n)] = \frac{1}{4\pi^2} \int_{\omega \in \mathbb{P}^2} \Phi_q(\omega) \mid 1 - G(\omega) \mid^2 \mid \tilde{W}(\omega) \mid^2 d\omega,$$

subject to the constraint that $G(\omega)$ be a strictly causal filter. Strict causality of $G(\omega)$ is required since it is located in the feedback branch of the error diffusion system.

The optimal choice of $G(\omega)$ has an intuitive interpretation, which is illustrated in Fig.4. Fig.4a shows the quantizing system together with the system, $\tilde{W}(\omega)$, and the perceived error, $\tilde{\varepsilon}(n)$. By exchanging $\tilde{W}(\omega)$ and $1 - G(\omega)$, Fig.4b illustrates that the filter $G(\omega)$ acts as a predictor for the signal $u(n)$. It should be emphasized that the signal $u(n)$ is introduced only to simplify our derivation and does not occur anywhere in the real system.

The problem of minimizing $E[\tilde{\varepsilon}^2(n)]$ is then equivalent to choosing an optimal linear predictor $G(\omega)$ for the stationary random process $u(n)$. This is a classical problem which

may be solved using $\Phi_u(\omega)$, the power spectrum of $u(n)$. If we assume that $q(n)$ is white, then

$$\begin{aligned} \Phi_u(\omega) &= \Phi_q(\omega) \mid \tilde{W}(\omega) \mid^2 \\ &= N_0 \mid \tilde{W}(\omega) \mid^2 . \end{aligned}$$

Appendix B gives the details of the optimized 2D linear predictor design for this problem.

2.3 Extension to Color Images

When applying error diffusion to color images, the input image is a sequence of vectors with a red (R), green (G) and blue (B) component, such that $s(n) = [r(n), g(n), b(n)]^T$. We will again assume that the three primary components are linearly proportional to light intensity. For this work quantization is performed separately on the RGB components. Other methods of quantization are possible, but separate quantization of RGB components does not lead to gamut mismatch.

A more natural color space to evaluate perception of the human visual system is spanned by a luminance-chrominance coordinate system. Experimental results are available [17, 19], describing the contrast sensitivity function of the human visual system to variations in luminance, as well as for variations in two chrominance components. For our experiments we use a color coordinate system specified by the primaries in Mullen's paper [17]. We write "Y" for luminance, "rg" for the red-green component and "yb" for the yellow-blue component. Furthermore, we selected the D_{6500} standard white point as the chromaticity of the luminance component.

Fig. 5 illustrates our color error diffusion algorithm, where the error diffusion is performed in the Y,rg,yb space, while the quantization is done in RGB coordinates. We define two transformation matrices A, B which respectively convert color coordinates from the RGB

space and from the Y,rg,yb coordinate system to standard X,Y,Z coordinates [20]. The matrix A is defined as

$$A = [\tilde{r}, \tilde{g}, \tilde{b}],$$

where $\tilde{r}, \tilde{g}$ and $\tilde{b}$ are column vectors, containing the X,Y,Z coordinates of the three primaries of the display device. These vectors have to be determined for each display. The matrix B can be calculated for the wavelengths of the primaries described in [17]. We obtained B to be

$$B = \begin{pmatrix} 0.0670 & -0.1116 & -0.0830 \\ 0.0707 & 0 & 0 \\ 0.0767 & 0.0049 & -1.0000 \end{pmatrix}.$$

Finally, define the transformation T to convert from RGB to Y,rg,yb coordinates as

$$T = B^{-1}A.$$

Later, we will see that this transformation decouples the optimal prediction equations so that one filter can be designed for each of the three color components.

The quantization error $q(n)$ is transformed to Y,rg,yb coordinates. Each component of the transformed quantization error is passed through a separate error diffusion filter. Then the filtered error is transformed back to RGB coordinates and added to the next unquantized input pixel.

The analysis of the system is analog to the case of luminance error diffusion, where signal variables now denote vectors of three color coordinates. The system functions $G(\omega)$ and $\tilde{W}(\omega)$ are now matrices of functions of spatial frequency. Including the color transformations T and T^{-1} of the feedback loop into the calculation, we obtain a relationship for the display error spectrum in terms of the quantization error spectrum,

$$E(\omega) = [I - T^{-1}G(\omega)T]Q(\omega),$$

where I is the identity matrix and T^{-1} denotes the inverse transformation from the luminance-chrominance to RGB coordinates.

A model for the monitor and the human visual system is shown in Fig. 6a. The components of the system are analog to the monochrome model. A transformation T is inserted, since $W(\Omega)$ is given for luminance-chrominance coordinates. We assume that human contrast sensitivity to variations in luminance and chrominance is decoupled, and that $W(\Omega)$ is therefore diagonal. If we also assume that $P(\Omega)$ and the D/A-conversion is the same for each of R,G and B, we may exchange the order of the system blocks and obtain the model illustrated in Fig. 6b. As shown earlier for the monochrome model, this system has a discrete equivalent, given in Fig. 6c, where

$$\tilde{W}(\omega)T = \begin{bmatrix} \tilde{W}_Y(\omega) & 0 & 0 \\ 0 & \tilde{W}_{rg}(\omega) & 0 \\ 0 & 0 & \tilde{W}_{by}(\omega) \end{bmatrix} T.$$

Fig. 7a shows the overall discrete color system. As illustrated in Fig. 7b, the spectrum of the perceived error is related to the spectrum of the quantization error by,

$$\begin{aligned} \tilde{\varepsilon}(\omega) &= \tilde{W}(\omega)T[I - T^{-1}G(\omega)T]Q(\omega) \\ &= \tilde{W}(\omega)[I - G(\omega)]TQ(\omega) \\ &= [I - \tilde{G}(\omega)]\tilde{W}(\omega)TQ(\omega), \end{aligned} \tag{4}$$

where

$$\tilde{G}(\omega) = \tilde{W}(\omega)G(\omega)\tilde{W}^{-1}(\omega). \tag{5}$$

Notice that $\tilde{G}(\omega)$ should be an optimal predictor for the signal $u(n)$. Therefore, the objective is to minimize the energy of $\tilde{\varepsilon}(n)$ by choosing the filter $\tilde{G}(\omega)$ and then converting to $G(\omega)$, using (5).

Let $\tilde{R}(m)$ be the autocorrelation matrix of the transformed quantization error, $\tilde{q}(n) = Tq(n)$. Then we will assume that

$$\begin{aligned} \tilde{R}(m) &= E[\tilde{q}(n+m)\tilde{q}^T(n)] \\ &= \tilde{R}_0\delta(m), \end{aligned} \tag{6}$$

where $\tilde{R}_0$ is assumed to be a diagonal matrix and $\delta(m)$ is the Dirac delta function, given by

$$\delta(m) = \begin{cases} 1 & \text{if } m = 0 \\ 0 & \text{otherwise.} \end{cases}$$

Again, the spatial independence of $\tilde{q}(n)$ is ensured by the methods described in Section 3. In general, the structure of $\tilde{R}_0$ is difficult to know when nonuniform quantization is used. If $\tilde{R}_0$ is not diagonal and the quantization error between components is correlated, we could calculate the optimal $G(\omega)$ according to a minimum mean square error criterion for the perceived error. However, this is a fairly complex problem, which involves the design of six error diffusion filters to account for the cross-coupling between the quantization error components. In practice, $\tilde{R}(m)$ is usually unknown, but our experiments indicate that the cross-correlation between the three error components is small.

Making the assumption of (6) we have that

$$\Phi_u(\omega) = \begin{bmatrix} \Phi_{u11}(\omega) & 0 & 0 \\ 0 & \Phi_{u22}(\omega) & 0 \\ 0 & 0 & \Phi_{u33}(\omega) \end{bmatrix}, \tag{7}$$

where

$$\Phi_{uii}(\omega) = \tilde{W}_{ii}(\omega) R_{0ii}.$$

By the form of (7), the three components of $u(n)$ are uncorrelated and the optimal predictor for $u(n)$ is therefore of the form

$$\begin{aligned} \tilde{G}(\omega) &= G(\omega) \\ &= \begin{bmatrix} G_{11}(\omega) & 0 & 0 \\ 0 & G_{22}(\omega) & 0 \\ 0 & 0 & G_{33}(\omega) \end{bmatrix}, \end{aligned}$$

where $G_{ii}(\omega)$ is chosen to be the optimal predictor for the signal $u_i(n)$ with power spectrum $\Phi_{uii}(\omega)$. Notice, that $\tilde{W}$ and $\tilde{W}^{-1}$ cancel in (5), since $W(\omega)$ and $G(\omega)$ are diagonal, and therefore $\tilde{G}(\omega) = G(\omega)$.

3 Whitening the Quantization Error Spectrum

3.1 Dithered Error Diffusion (DED)

The design of the error diffusion filter assumed that the quantization error, $q(n)$, has a white power spectrum. However, simulations showed that this assumption is not always valid. Based on our simulations, two observations about the power spectrum of $q(n)$ were made. On the one hand, the whiteness of $q(n)$ depends on the error diffusion filter. On the other hand, the simulations indicated that the quantization error is not white in regions of the image, where the input gray scale value is close to one of the quantization levels.

In Appendix C, we show that a possible way to obtain a white quantization error spectrum is to randomly vary the thresholds, $t(n)$, of the quantizer, Q. Moreover it is shown that the expected value of the output image, $E[Q[\tilde{s}(n)]]$, is equal to the expected value of the quantizer input, $E[\tilde{s}(n)]$ and that the signal is uncorrelated from $q(n)$. Let α_k for $k = 0 \ldots M-1$ be the M nonuniformly spaced quantization levels, and assume that the signal falls in the range $\alpha_0 \leq s(n) \leq \alpha_{M-1}$. The dithered quantization of $s(n)$ is given by

$$y(n) = \tilde{Q}[s(n)] = \begin{cases} \alpha_{k-1} & \text{if } \alpha_{k-1} \leq s(n) < t(n) \\ \alpha_k & \text{if } t(n) \leq s(n) < \alpha_k \end{cases}$$

where $t(n)$ is a sequence of independent random thresholds uniformly distributed on $[\alpha_{k-1}, \alpha_k]$.

We also show in Appendix C that for a uniform quantizer the variation of the thresholds is equivalent to adding noise to the signal before it is quantized. This is done by defining a noise sequence, $N(n)$, of independent random variables. Each N is uniformly distributed on the interval $[-\Delta q/2; \Delta q/2]$. As for the nonuniform quantizer, the expected value of the output image, $E[Q[\tilde{s}(n)]]$, is equal to the expected value of the quantizer input, $E[\tilde{s}(n)]$, and the signal is uncorrelated from the noise. Fig. 8 illustrates the resulting quantization system. We will refer to this method as "Dithered Error Diffusion" (DED).

Fig. 9 shows estimates of the power spectrum of the quantization error obtained for a natural image using the Floyd-Steinberg filter and an optimized error diffusion filter. The estimates of the power spectrum are calculated by averaging periodograms over the image. They are plotted as a function of f_1, while f_2 is set to zero. We used a uniform 3 bit quantizer and limited the input signal to the range of the quantizer to avoid saturation effects. A comparison of the spectra, resulting from the basic error diffusion method and the DED algorithm clearly shows the whitening effect of the DED algorithm when the Floyd-Steinberg filter is used. We also notice that the optimized error diffusion filter produces a white quantization error with or without the addition of dithering noise. However, the disadvantage of the DED algorithm is an overall increase of graininess and noise in the output image.

3.2 Locally Dithered Error Diffusion (LDED)

To reduce the noise energy, we selectively add noise to the image based on a nearest neighbor criterion. We will call this method "Locally Dithered Error Diffusion" (LDED). Fig. 10 illustrates the algorithm. Our simulations indicate, that areas with smooth, slowly varying gray scale values in the input image often show artificial contouring after they are quantized. This may be due to the fact, that most pixels in a neighborhood in the input image are represented by the same quantization level and that the diffused error is too small to change the quantization level of successive pixels. As a result, the quantization error tends to have the same sign in such areas which correspond to a DC component in the quantization error spectrum. Furthermore, the quantization levels in the output image change abruptly. Therefore, it seems to be desirable, to whiten the quantization error by adding some noise in critical regions of the image. As a criterion, the algorithm compares the quantization levels of two previously quantized pixels, located to the left and above the current input pixel, such that

```
if (y(n1-1,n2) = y(n1,n2-1))
   add noise
else
   do not add noise.
```

Whenever the same quantization level was assigned to these two pixels, noise of the same kind as above is added to the input pixel. This modification reduces the variance of the quantization error, but also whitens the quantization error in critical regions of the image.

4 Models for the Human Visual System

4.1 Luminance Contrast Sensitivity

In this Section, we will briefly describe two of the various human MTF models found in the literature, and then develop the model used in our experiments. Most models for the human MTF have a lowpass characteristic. It should be emphasized that our proposed method for designing an optimal error diffusion filter for a given visual model is applicable to any given modulation transfer function describing the specific display and viewing conditions.

Sullivan, Ray and Miller [14, 15] quote a model from Daly that describes the human MTF by a weighted exponential function of the frequency vector. The model is also a function of the viewing angle and decreases faster for diagonal frequencies, to account for the reduced sensitivity of the human visual system toward luminance changes in diagonal directions.

Näsänen [16] describes a circular symmetric model based on an exponential function. This model features parameters, which depend on the average luminance of the display. The slope of the exponential decreases with increasing average luminance.

For our simulations, a model was used that combines the models from Sullivan et al. and

Näsänen. Our model is based on an exponential function as used by Näsänen [16]

$$W(\tilde{f}) = K(L)\exp[-\alpha(L)\tilde{f}],$$

where L is the average luminance in cd/m^2, $\tilde{f}$ is the spatial frequency in cycles/degree,

$$\begin{aligned} K(L) &= aL^b, \\ \alpha(L) &= \frac{1}{c\ln(L)+d}, \end{aligned}$$

and $a = 131.6, b = 0.3188, c = 0.525, d = 3.91$. Deviating from Näsänen's model, we define $\tilde{f}$ to be the weighted magnitude of the frequency vector $f = (f_1, f_2)$, where the weighting has an angular dependence as used by Sullivan [14],

$$\tilde{f} = \frac{\parallel f \parallel}{s(\Theta)},$$

where $\parallel f \parallel = \sqrt{f_1^2 + f_2^2}$ and

$$s(\Theta) = \frac{1-w}{2}\cos(4\Theta) + \frac{1+w}{2}.$$

The angle Θ is defined as

$$\Theta = \arctan(\frac{f_1}{f_2})$$

and the symmetry parameter $w = 0.7$. Throughout our simulations, we assumed a monitor MTF, $P(\Omega) = 1$. An investigation of the spatial characteristics of grayscale CRT pixels was recently presented by Naiman and Makous [21].

4.2 Chrominance Contrast Sensitivity

We base our model for human sensitivity toward variations in chrominance on the experimental results obtained by Mullen [17]. Evaluating the presented data, the chrominance contrast sensitivity function can be approximated by an exponential function,

$$W(f) = A\exp(-\alpha\tilde{f}).$$

We determined $\alpha = 0.419$, $A = 100$ for both chrominance components and assumed circular symmetry for our model such that $\tilde{f} = \sqrt{f_1^2 + f_2^2}$. As with the luminance model, we assume $P(\Omega) = 1$ for both chrominance components.

5 Experimental Results

5.1 Error Diffusion in Luminance

Our experiments were carried out on a Sun Sparc Station 1. Simulations were performed with 512 by 512 pixel natural images and a gray scale ramp. A monochrome version of a natural color image was obtained by calculating the luminance component, Y, according to the Y,cr,cb standard [20] from RGB image data. The monochrome image was then scaled and rounded to integer values between 0 and 255. Uniform and nonuniform quantizers were examined. We chose to use a nonuniform quantizer where steps increase toward higher luminance levels since this corresponds to the fact expressed in Weber's Law that human contrast sensitivity follows a logarithmic function of luminance. Let $\alpha_{Y,k}$ denote the luminance quantization levels, where a value of 0 corresponds to zero intensity, 255 denotes maximal intensity and intermediate values are proportional to energy of the corresponding image pixel. The luminance quantization levels were assigned such that

$$\alpha_{Y,k} = 255(k/7)^{1.8},$$

where $k = 0 \ldots 7$.

Our output images were displayed on an 8 bit color monitor. We calibrated the monitor using measured values of gamma and offset. The error diffused image was transformed according to the nonlinearity of the display. A normal viewing distance was assumed and measured to be 40cm, which is equivalent to approximately 3.5 times the image height. The quantized images shown in this paper are zoomed by a factor of 2 and should therefore be

viewed at a distance of approximately 7 times the image height. Calculating the angle of perception for a single pixel yields $\Delta\phi = 0.0317^o$/pixel. This determines the sampling rate, $f_s = (\Delta\phi)^{-1} = 31.5$ cycles/degree. The average luminance of our display was measured to be approximately $L = 11.0cd/m^2$.

The coefficients for the first order linear prediction filters for luminance and chrominance are listed in Tab. 1. Notice that the coefficient $g_{1,1}$ of both prediction filters is negative and that the coefficients don't sum to one. Since the optimized filters shape the display error spectrum according to a human visual model, some display error energy is allowed at zero frequency. Notice also that the coefficient $g_{-1,1}$ is very close to zero and can be neglected to reduce the computational complexity of the algorithm.

Fig. 11a and Fig. 11b show a quantized gray scale ramp, comparing the performance of the basic error diffusion algorithm, using the Floyd-Steinberg filter and the first order linear predictor for luminance, according to the human visual model described in Section 4. When using the Floyd-Steinberg filter the quantized image shows diagonal patterns and artificial contours. Applying a first order linear predictor with the basic error diffusion shows less patterns.

Our simulation indicated that averaged over the entire image the quantization error spectrum is whiter when using a linear prediction filter than for the alternative filters (see Fig. 9). This may result from limit cycles and saturation effects, which occur more frequently for filters with coefficients that sum to one. For all tested filters the quantization error is not equally white in all regions of the image. Whenever the input gray scale value is close to a quantization level, the whiteness assumption seems to be locally violated. In these regions, the contribution of the quantization errors of adjacent pixels to the current pixel is negligible. Thus, the quantizer assigns the same output gray level to almost all pixels in that region. This causes artifacts that are visible as lines in the gray scale ramp.

Fig. 11c shows the the resulting image for the DED algorithm using the first order linear predictor. The resulting image does not suffer from lines and patterns as the previous two examples. However, the overall perception of the image is more noisy.

Fig. 11d shows the resulting image for the LDED algorithm. This algorithm also removes the false contours but the LDED algorithm is superior to the DED algorithm, since it reduces the amount of noise in the image.

Fig. 12 shows the same algorithms applied to a natural image. Critical regions of the image such as the shoulder and the cheek appear to be smoother for the LDED algorithm than for basic error diffusion, using either the Floyd Steinberg filter, or the optimal linear predictor.

Knox [9] proposed to display the quantization error image to examine the correlation between the input image and the quantization error. Fig. 13a shows the quantization error image, for a natural image, processed with basic error diffusion, using the Floyd-Steinberg filter. It can be seen that the quantization error is highly correlated with the input image. Fig. 13b shows the quantization error image for the same natural image, processed with our optimized error diffusion algorithm. Notice, that the quantization error becomes less correlated to the input image simply, by changing the coefficients of the error diffusion filter. The whitening effect of adding dithering noise can be seen in Fig. 13c and d, which show the quantization error images for DED and LDED. Adding dithering noise globally to the image produces a quantization error that is almost uncorrelated. The LDED algorithm improves the whiteness of the quantization error without adding an excessive amount of noise.

5.2 Color Error Diffusion

Our images were quantized in RGB coordinates, using 256 colors, where we assigned 3 bits (8 levels) to red, 3 bits to green and 2 bits (4 levels) to blue. Our input data is linear in luminance. Again, uniform and non-uniform quantizers were examined, where a nonuniform quantizer was chosen with increasing steps toward higher luminance levels. Let $\alpha_{r,k}, \alpha_{g,k}$ and $\alpha_{b,k}$ denote the R,G and B quantization levels respectively, where a value of 0 corresponds to zero intensity, 255 denotes maximal intensity and intermediate values are proportional to energy of the corresponding primary. For red and green the quantization levels were assigned such that

$$\alpha_{r,k} = \alpha_{g,k} = 255(k/7)^{1.8},$$

where $k = 0 \ldots 7$. For the blue primary we used

$$\alpha_{b,k} = 255(k/3)^{1.8},$$

where $k = 0 \ldots 3$. The display and viewing conditions were the same as for the monochrome case.

Fig. 14 illustrates the results, when applying basic error diffusion with the Floyd-Steinberg filter and optimized error diffusion to a color image. As for luminance error diffusion, the optimized algorithm removes almost all artificial contouring in smooth areas of the image. Furthermore it eliminates deterministic patterns typically associated with the Floyd-Steinberg filter.

Fig. 15 shows the Y-component of the quantization error images for a natural color image. As for error diffusion in luminance, the correlation between the input image and the quantization error is greatly reduced, when using an optimized error diffusion filter. However, Fig. 15c and d show that the contours of the original image are still noticeable, even when dithering noise is added to the quantizer input. This results from saturation of

the quantizer, mainly for the blue component, since only four output levels are assigned to this component and the white quantization error assumption is often violated.

6 Conclusion

Starting with an analysis of the basic error diffusion algorithm proposed by Floyd and Steinberg, we developed an optimization criterion for the design of an error diffusion filter for monochrome images, based on a model for the human visual system. We showed that the analysis can also be extended to color images. Additive white noise is used to ensure a white quantization error spectrum, which is an important underlying assumption for the design of the error diffusion filter. The resulting images show less artificial contouring and a uniform texture. In addition, the noise in slowly varying regions of the image appears to be more uncorrelated and less noticeable.

Acknowledgement

The author would like to thank the Eastman Kodak Company for the use of their image "balloon" for the experiments.

A Appendix

In this section we will show that $E[\varepsilon^2(x)] = E[\tilde{\varepsilon}^2(n)]$, where

$$E[\tilde{\varepsilon}^2(n)] = \frac{1}{4\pi^2} \int_{\omega \in I\!P^2} \Phi_e(\omega) \mid \tilde{W}(\omega) \mid^2 d\omega$$

and $I\!P = [-\pi, \pi]$.

$E[\varepsilon^2(x)]$ is given by

$$E[\varepsilon^2(x)] = \frac{1}{4\pi^2} \int_{\Omega \in I\!R^2} \Phi_\varepsilon(\Omega) d\Omega, \tag{8}$$

where $\Omega = (\Omega_1, \Omega_2)$ is a frequency vector with $\Omega_1, \Omega_2 \in (-\infty, \infty)$. The digital image is displayed and converted to a spatially continuous signal. It is filtered by the monitor modulation transfer function $P(\Omega)$. Ideally we would like $P(\Omega)$ to be a perfect lowpass with

$$P(\Omega) = \begin{cases} 1 & \text{if } \Omega \in I\!D^2 \\ 0 & \text{otherwise,} \end{cases}$$

where $I\!D = [-\pi f_s, \pi f_s]$, and f_s is the sampling frequency of the monitor. Since the monitor is not ideal, we also have to consider effects due to the side lobes of $P(\Omega)$. Accounting also for the effect of the human MTF, $W(\Omega)$, we obtain the power spectrum of the perceived error, $\Phi_\varepsilon(\Omega)$, in terms of the display error power spectrum, $\Phi_e(\Omega/f_s)$

$$\Phi_\varepsilon(\Omega) = \Phi_e\left(\frac{\Omega}{f_s}\right) \mid P(\Omega)W(\Omega) \mid^2 .$$

We note that $\Phi_e(\Omega/f_s)$ is the power spectrum of a discrete signal and is therefore a 2D periodic function with period 2π. Substituting in (8) and expanding the integral we obtain

$$\begin{aligned} E[\varepsilon^2(x)] &= \frac{1}{4\pi^2} \int_{\Omega \in I\!R^2} \Phi_e(\frac{\Omega}{f_s}) \mid P(\Omega)W(\Omega) \mid^2 d\Omega \\ &= \frac{1}{4\pi^2} \sum_{l \in Z\!\!Z^2} \int_{\Omega \in I\!D^2} \Phi_e(\frac{\Omega}{f_s} + 2\pi l) \mid P(\Omega + 2\pi l f_s)W(\Omega + 2\pi l f_s) \mid^2 d\Omega, \end{aligned}$$

where $l = (l_1, l_2)$ and $Z\!\!Z$ is the set of all integers. Exchanging the order of the sum and the integral and using the periodicity of $\Phi_e(\Omega/f_s)$, we have

$$E[\varepsilon^2(x)] = \frac{1}{4\pi^2} \int_{\Omega \in I\!D^2} \Phi_e(\frac{\Omega}{f_s}) \sum_{l \in Z\!\!Z^2} \mid P(\Omega + 2\pi l f_s)W(\Omega + 2\pi l f_s) \mid^2 d\Omega.$$

Finally we make the substitution $\omega = \Omega/f_s$ to obtain

$$\begin{aligned} E[\varepsilon^2(x)] &= \frac{1}{4\pi^2} \int_{\omega \in I\!P^2} \Phi_e(\omega) f_s^2 \sum_{l \in Z\!\!Z^2} \mid P(\omega f_s + 2\pi l f_s)W(\omega f_s + 2\pi l f_s) \mid^2 d\omega \\ &= \frac{1}{4\pi^2} \int_{\omega \in I\!P^2} \Phi_e(\omega) \mid \tilde{W}(\omega) \mid^2 d\omega \\ &= E[\tilde{\varepsilon}^2(n)], \end{aligned}$$

where $\tilde{W}(\omega)$ is any discrete space filter, which satisfies

$$\mid \tilde{W}(\omega) \mid^2 = f_s^2 \sum_{l \in \mathbb{Z}^2} \mid P(\omega f_s + 2\pi l f_s) W(\omega f_s + 2\pi l f_s) \mid^2 .$$

B Appendix

In this Section we will develop linear predictor equations for the 2D random process, $u(n)$. The signal $u(n)$ is the output of the linear system $\tilde{W}(\omega)$. Since the input of the system is a stationary white noise signal, $q(n)$, with power spectral density N_0, the output, $u(n)$, is also stationary. The power spectral density of $u(n)$ is given by

$$\Phi_u(\omega) = N_0 \mid \tilde{W}(\omega) \mid^2 . \tag{9}$$

Assuming raster order when processing the input image, each present pixel divides the image into a past and future halfplane as illustrated in Fig. 16. Based on pixels from the past (causal) halfplane of the signal, we want to obtain an estimate of the present pixel, that is optimal in the mean square sense. Let $u_{0,0}$ denote the present pixel. Then we define $u_{k,l}$ to be the pixel l steps to the right and k steps below the present pixel. An estimate of the present pixel, $\tilde{u}_{0,0}$, in terms of weighted previous pixels is given by

$$\tilde{u}_{0,0} = \sum_{l=1}^{p} h_{0,l} u_{0,-l} + \sum_{k=1}^{p} \sum_{l=-p}^{p} h_{k,l} u_{-k,-l},$$

where $h_{k,l}$ denote the coefficients of a p-th order, 2D, causal filter. Define U to be a vector of image pixels with

$$U^T = [u_{0,-1}, .., u_{0,-p}, u_{-1,p}, .., u_{-1,-p}, .., u_{-p,p}, .., u_{-p,-p}],$$

where T denotes the transpose of the vector. The dimension of U is $2(p^2 + p)$. Then let

$$h = [h_{0,1}, .., h_{0,p}, h_{1,-p}, .., h_{1,p}, ..., h_{p,-p}, .., h_{p,p}].$$

Using these definitions we can write for $\tilde{u}_{0,0}$

$$\tilde{u}_{0,0} = hU.$$

The coefficients of h that form the MMSE estimator for $\tilde{u}_{0,0}$ are given by

$$h = R_u^{-1} b,$$

where $b = E[u_{0,0}U^T]$ and $R_u = E[UU^T]$. R_u is the autocorrelation matrix of U. Notice that R_u has a structure known as Block Toeplitz. Let the point spread functions of the monitor and the human visual system be denoted by $p(x)$ and $w(x)$. Then the coefficients of b and R_u can be obtained by calculating and sampling the autocorrelation function, $r_u(x)$, of the convolution of $p(x)$ and w(x),

$$\begin{aligned} r_u(x) &= N_0 p(x) * p(-x) * w(x) * w(-x) \\ &= N_0 \mathcal{F}^{-1}[\mid P(\Omega)W(\Omega) \mid^2], \end{aligned}$$

and $\mathcal{F}^{-1}$ denotes the inverse Fourier Transform. We can approximate $r_u(x)$ by

$$r_u(x) \approx \Delta f^2 \sum_{k \in \mathbb{Z}^2} \mid P(k\Delta f)W(k\Delta f) \mid^2 \exp[j2\pi k \Delta f x],$$

where Δf is sufficiently small. To obtain the coefficients of R_u, $r_u(x)$ is sampled at multiples of the spacing between adjacent pixels, Δx, with

$$E[u_n u_m] = r_u((n-m)\Delta x).$$

C Appendix

We will show that dithered quantization of a signal, $s(n)$, will generate quantization error, $q(n)$, which is zero mean, white and uncorrelated from the signal, $s(n)$.

Let α_k for $k = 0 \ldots M-1$ be the M nonuniformly spaced quantization levels, and assume that the signal falls in the range $\alpha_0 \leq s(n) \leq \alpha_{M-1}$. The dithered quantization of $s(n)$ is given by

$$y(n) = \tilde{Q}[s(n)] = \begin{cases} \alpha_{k-1} & \text{if } \alpha_{k-1} \leq s(n) < t(n) \\ \alpha_k & \text{if } t(n) \leq s(n) < \alpha_k \end{cases}$$

where $t(n)$ is a sequence of independent random thresholds uniformly distributed on $[\alpha_{k-1}, \alpha_k]$. Notice that in the case of uniform quantization with spacing $\Delta\alpha$, this corresponds to the simple operation

$$y(n) = Q[s(n) + N(n)]$$

where $Q[\cdot]$ is normal minimum distance quantization, and $N(n)$ is a sequence of independent noise samples with uniform distribution on $[-\Delta\alpha/2, \Delta\alpha/2]$.

The quantization error is given by $q(n) = s(n) - y(n)$. We first compute the conditional mean of the quantization error given the signal.

$$\begin{aligned} E[q(n)|s(n)] &= E[s(n) - y(n)|s(n)] \\ &= s(n) - E[\tilde{Q}[s(n)]|s(n)] \\ &= s(n) - \alpha_{k-1}\frac{\alpha_k - s(n)}{\alpha_k - \alpha_{k-1}} + \alpha_k\frac{s(n) - \alpha_{k-1}}{\alpha_k - \alpha_{k-1}} \\ &= s(n) - s(n) \\ &= 0 \end{aligned}$$

From this we may show that $q(n)$ is mean zero

$$E[q(n)] = E[E[q(n)|s(n)]] = 0$$

and uncorrelated for $n \neq m$.

$$\begin{aligned} E[q(n)q(m)] &= E[E[q(n)q(m)|s(n)s(m)]] \\ &= E[E[q(n)|s(n)]E[q(m)|s(m)]] \\ &= 0 \end{aligned}$$

The variance of $q(n)$ is given by

$$\begin{aligned} E[(q(n))^2] &= E[E[(q(n))^2]|s(n)]] \\ &= E\left[(s(n) - \alpha_{k-1})^2\frac{\alpha_k - s(n)}{\alpha_k - \alpha_{k-1}} + (\alpha_k - s(n))^2\frac{s(n) - \alpha_{k-1}}{\alpha_k - \alpha_{k-1}}\right] \end{aligned}$$

$$
\begin{aligned}
&= E[(s(n) - \alpha_{k-1})(\alpha_k - s(n))] \\
&= \text{constant} = N_0
\end{aligned}
$$

Therefore, $q(n)$ has autocorrelation

$$
E[q(n)q(m)] = \begin{cases} N_0 & \text{if } m = n \\ 0 & \text{otherwise} \end{cases}
$$

Finally, $q(n)$ and $s(m)$ are uncorrelated for all n and m.

$$
\begin{aligned}
E[q(n)s(m)] &= E[E[q(n)s(m)|s(m)]] \\
&= E[s(m)E[q(n)|s(m)]] \\
&= E[s(m)0] = 0
\end{aligned}
$$

References

[1] R. W. Floyd and L. Steinberg, "An Adaptive Algorithm for Spatial Greyscale," *Proc. SID, vol.17, no.2, pp.75-77, 1976.*

[2] E. Barnard, "Optimal error diffusion for computer-generated holograms," *J. Opt. Soc. Am. A/vol.5, no.11, pp.1803 - 1817, 1988.*

[3] C. A. Bouman, M. T. Orchard, "Color Image Display with a Limited Palette Size," *Proc. SPIE Conf. Visual Commun. Image Processing (Philadelphia, PA), pp.522-533, Nov.8-10, 1989.*

[4] M. T. Orchard, C. A. Bouman, "Color Quantization of Images," *IEEE Trans. Signal Processing, vol. 39, no. 12, pp.2677 - 2690, 1991.*

[5] C. Billotet-Hoffmann, O. Bryngdahl, "On Error Diffusion Technique for Electronic Halftoning," *Proc. SID, vol. 24/3, 1983, pp.253 - 258.*

[6] R. A. Ulichney, "Dithering with Blue Noise," *Proc. IEEE, vol.76, no.1, pp.56-79, 1988.*

[7] G. Goertzel, G. R. Thompson, "Digital Halftoning on the IBM 4250 Printer," *IBM J. Res. Develop. vol. 31, no. 1, pp.2 - 15, 1987.*

[8] G. Goertzel and G. R. Thompson, " 'Halftoning' Techniques for Displaying Images with a Limited Color Palette," *EI West 1990, Pasadena, CA, pp.102-108.*

[9] K. T. Knox, " Error Image in Error Diffusion," *Proc. SPIE Conf. Electronic Imaging, (San Jose, CA), Feb.9-14, 1992.*

[10] J. Sullivan, R. Miller, "A New Algorithm for Image Halftoning Using a Human Visual Model." *SPSE 43rd Annual Meeting, Rochester, NY (1990), pp. 145 - 148*

[11] R. Miller, J. Sullivan, "Color Halftoning Using Error Diffusion and a Human Visual System Model." *SPSE 43rd Annual Meeting, Rochester, NY (1990), pp. 149 - 152*

[12] B. Girod, H. Almer, L. Bengtsson, B. Christensson, P. Weiss, "A Subjective Evaluation of Noise-Shaping Quantization for Adaptive Intra-/Interframe DPCM Coding of Color Television Signals," *IEEE Trans. Communications, vol. 36, no.3, March 1988, pp. 332 - 346.*

[13] T. Pappas, D. L. Neuhoff, "Least-Squares Model-Based Halftoning," *Proc. SPIE Conf. Electronic Imaging, (San Jose, CA), Feb.9-14, 1992.*

[14] J. Sullivan, L. Ray, R. Miller, "Design of Minimum Visual Modulation Halftone Patterns," *IEEE Trans. Syst., Man, Cybernetics, vol.21, no.1, 1991.*

[15] J. Sullivan, R. Miller, G. Pios "Image Halftoning Using Visual Error Diffusion," *Submitted for publication.*

[16] R. Näsänen, "Visibility of Halftone Dot Textures," *IEEE Trans. Syst., Man, Cybernetics, vol. SMC-14, no.6, 1984.*

[17] K. T. Mullen, "The Contrast Sensitivity of Human Color Vision to Red-Green and Blue-Yellow Chromatic Gratings," *J. Physiol. 359, 1985, pp. 381 - 400.*

[18] J. G. Proakis, D. G. Manolakis, *Introduction to Digital Signal Processing,* Macmillan Publishing Company, New York, 1988.

[19] S. A. Rajala, H. J. Trussel, B. Krishnakumar, "Visual Sensitivity to Color-Varying Stimuli," *Proc. SPIE Conf. Electronic Imaging, (San Jose, CA), Feb.9-14, 1992.*

[20] A. N. Netravali, B. G. Haskell, *Digital Pictures,* Plenum Press, New York and London, 1988.

[21] A. C. Naiman, W. Makous, "Spatial non-linearities of grayscale CRT pixels," *Proc. SPIE Conf. Electronic Imaging, (San Jose, CA), Feb.9-14, 1992.*

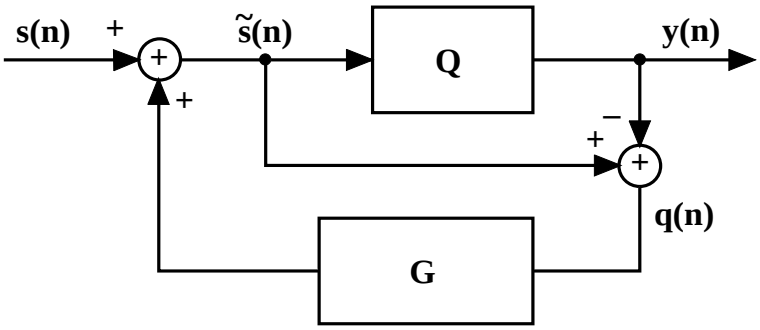

Figure 1: Block diagram of the basic error diffusion algorithm.

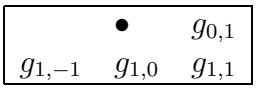

Figure 2: Location of the filter coefficients.

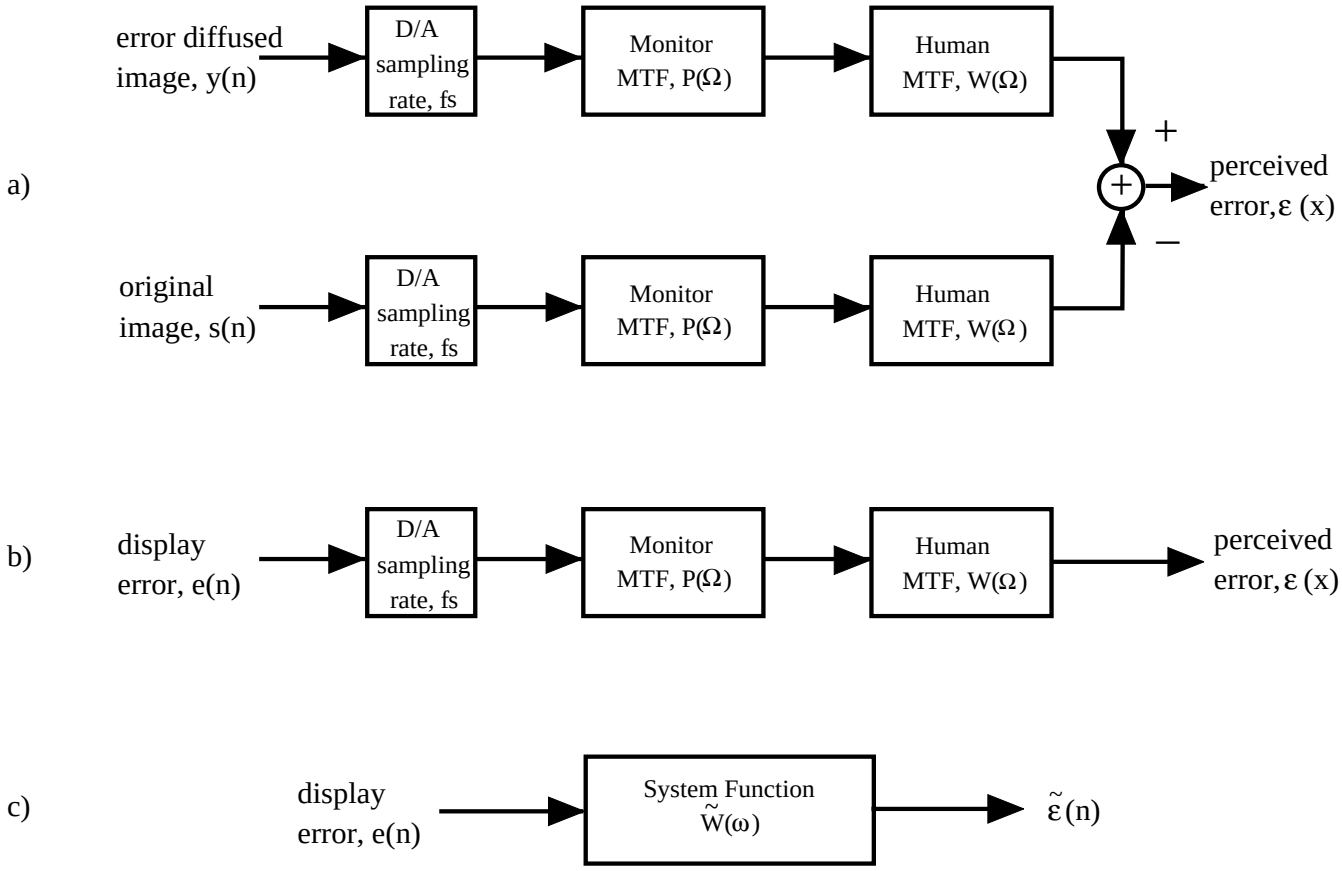

Figure 3: Block diagram of the monitor and the human visual system.

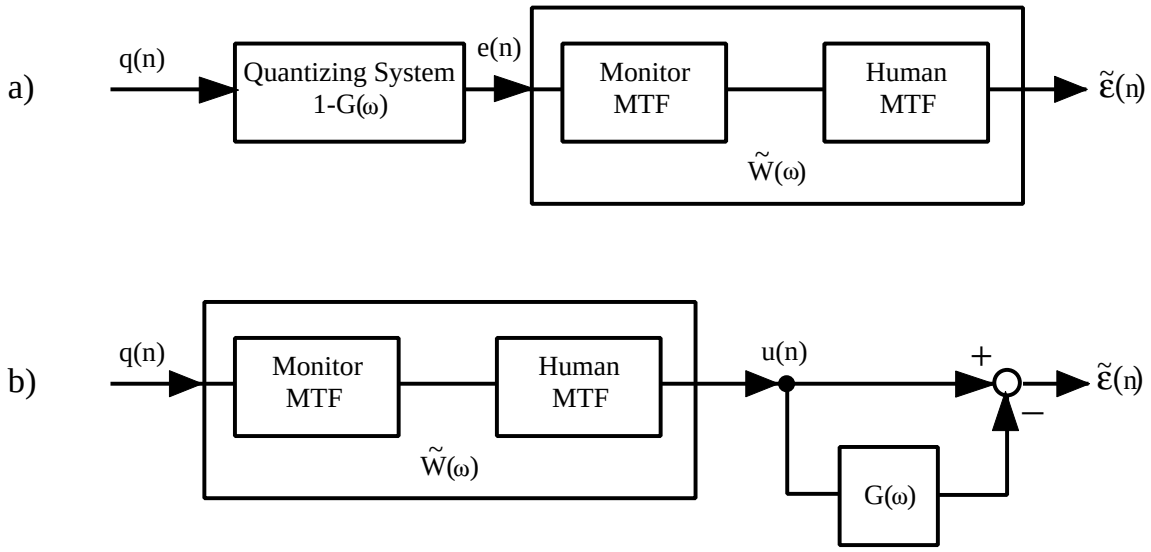

Figure 4: Block diagram of the overall system.

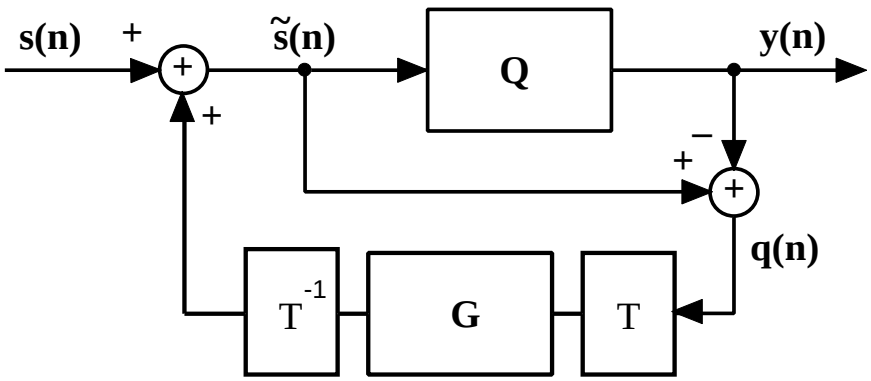

Figure 5: Block diagram of the error diffusion algorithm applied to color images.

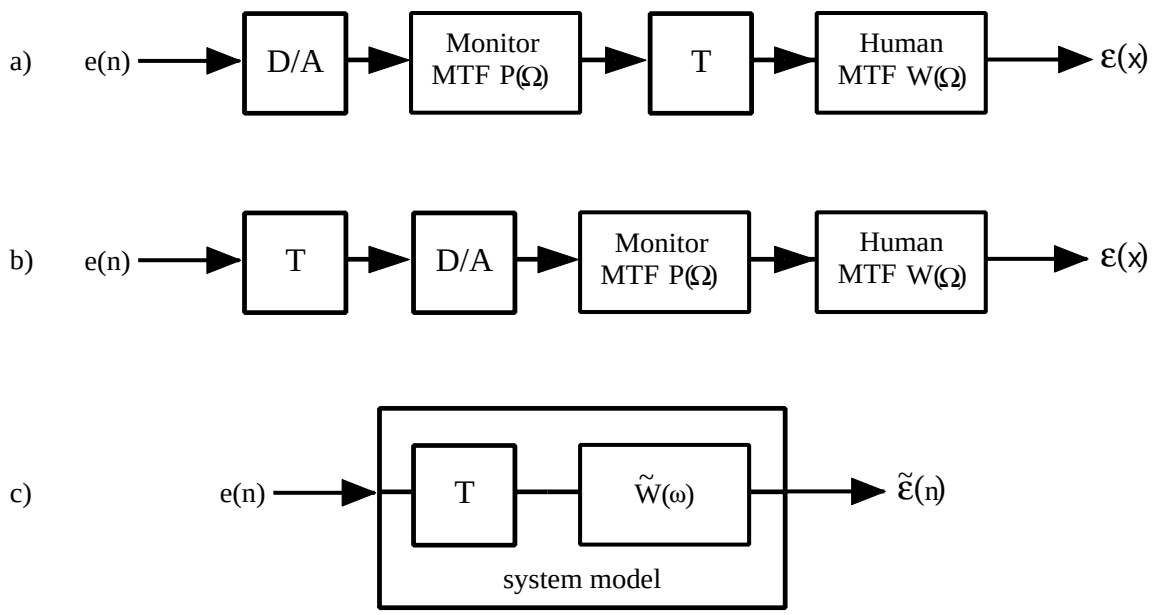

Figure 6: Block diagram of the monitor and visual system.

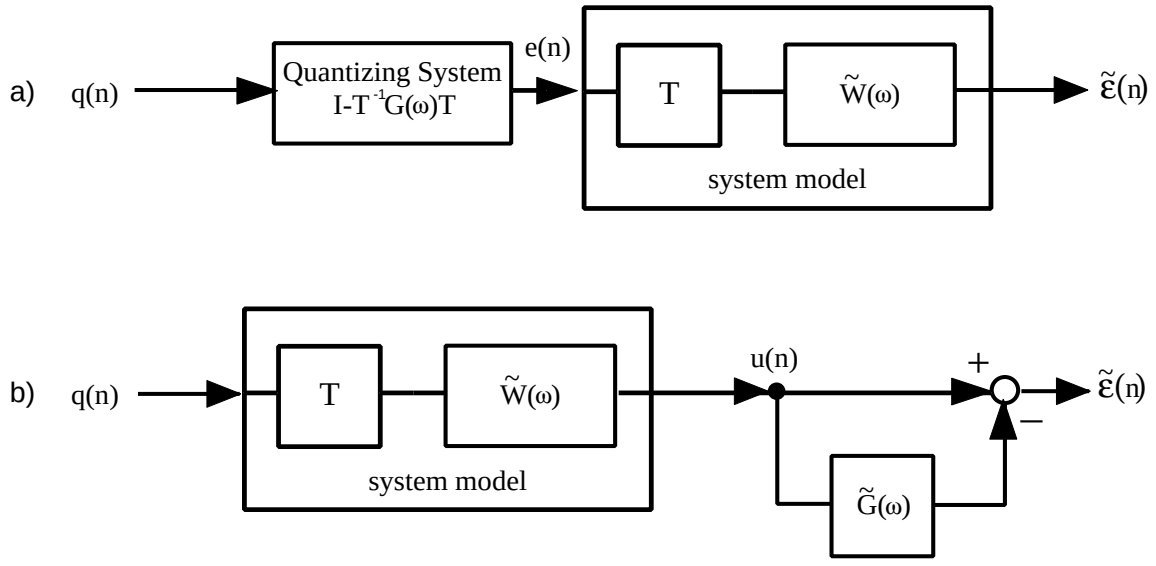

Figure 7: Block diagram of the overall color system.

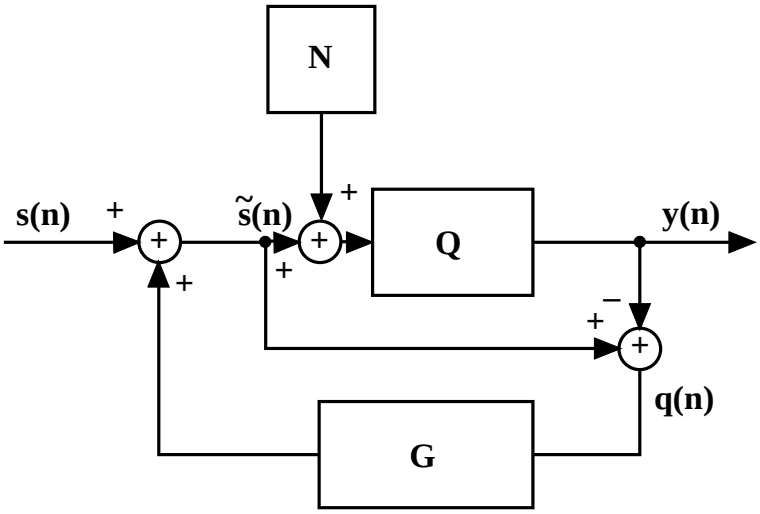

Figure 8: Block diagram of the dithered error diffusion algorithm.

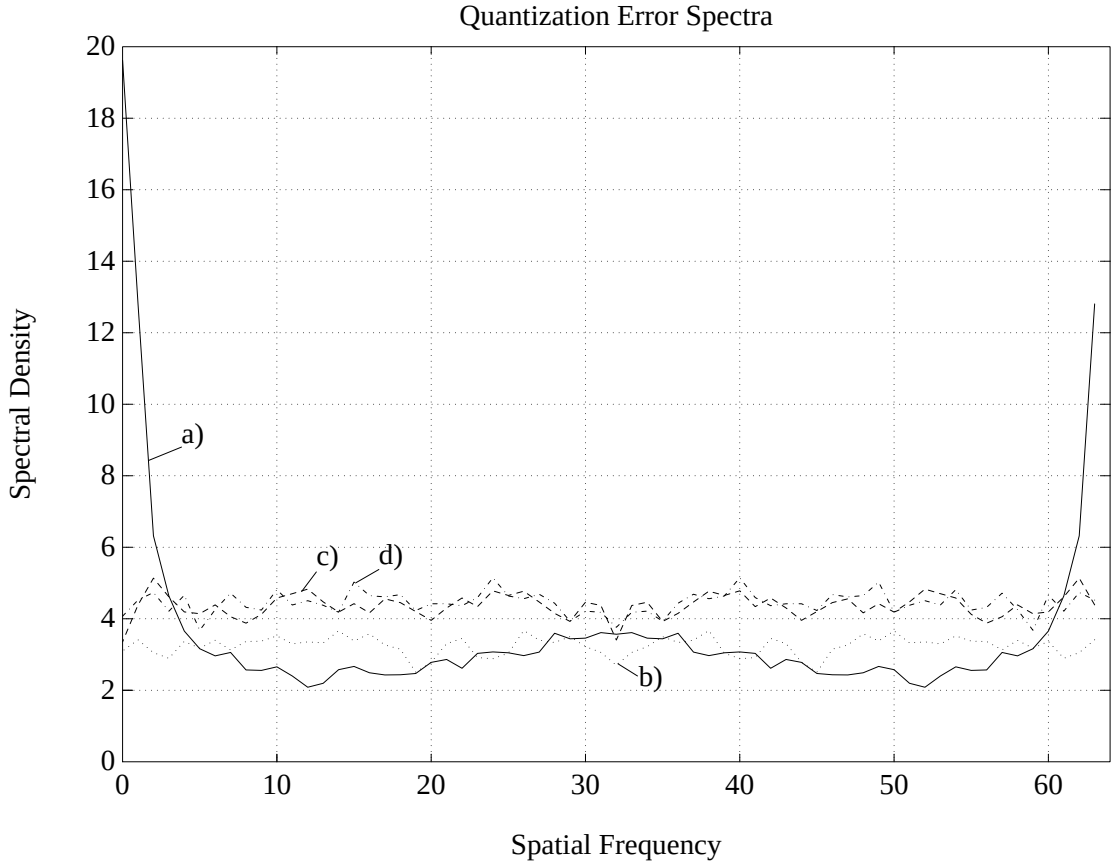

Figure 9: Estimates of the power spectrum of the quantization error as a function of f_1 and $f_2 = 0$: a)Basic error diffusion: Floyd-Steinberg filter; b)Basic error diffusion: Linear predictor; c)Dithered error diffusion: Floyd-Steinberg filter; d)Dithered error diffusion: Linear predictor.

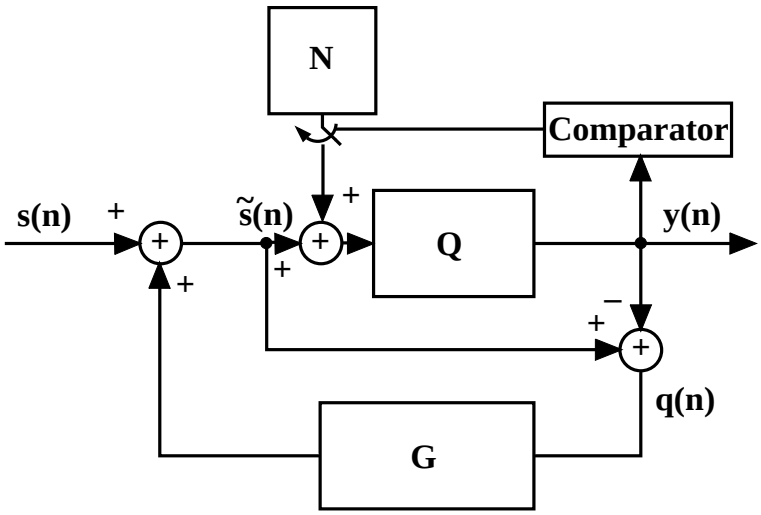

Figure 10: Block diagram of the locally dithered error diffusion algorithm.

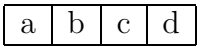

Figure 11: Error diffusion applied to a gray scale ramp. a) Basic error diffusion: Floyd-Steinberg filter. b) Basic error diffusion: 1st order linear predictor. c) Dithered error diffusion (DED): 1st order linear predictor. d) Locally dithered error diffusion (LDED): 1st order linear predictor.

a	b
c	d

Figure 12: Error diffusion applied to a natural image. a) Basic error diffusion: Floyd-Steinberg filter. b) Basic error diffusion: 1st order linear predictor. c) Dithered error diffusion (DED): 1st order linear predictor. d) Locally dithered error diffusion (LDED): 1st order linear predictor.

a	b
c	d

Figure 13: Quantization error images for a natural image. a) Basic error diffusion: Floyd-Steinberg filter. b) Basic error diffusion: 1st order linear predictor. c) Dithered error diffusion (DED): 1st order linear predictor. d) Locally dithered error diffusion (LDED): 1st order linear predictor.

a	b
c	d

Figure 14: Color error diffusion applied to the natural image "Balloon". a) Basic error diffusion: Floyd-Steinberg filter. b) Basic error diffusion: 1st order linear predictor. c) Dithered error diffusion (DED): 1st order linear predictor. d) Locally dithered error diffusion (LDED): 1st order linear predictor.

a	b
c	d

Figure 15: Luminance quantization error for "Balloon". a) Basic error diffusion: Floyd-Steinberg filter. b) Basic error diffusion: 1st order linear predictor. c) Dithered error diffusion (DED): 1st order linear predictor. d) Locally dithered error diffusion (LDED): 1st order linear predictor.

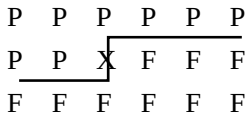

Figure 16: P=Past and F=Future halfplanes of the image. X denotes the present pixel.